Research Article | Vol. 9, No. 3 | 1 Mar 2019 | OPTICAL MATERIALS EXPRESS 1033
Optical Materials EXPRESS

Colorful multifunctional surfaces produced by femtosecond laser pulses

ERIK M. GARCELL[1] AND CHUNLEI GUO[1,2,*]

[1]The Institute of Optics, University of Rochester, Rochester, NY 14627, USA
[2]Changchun Institute of Optics, Fine Mechanics, and Physics, Changchun 130033, China
[*]guo@optics.rochester.com

Abstract: Femtosecond laser ablation of materials can alter their optical, chemical, electrical, and mechanical properties. It has been previously shown that ablated metals can be simultaneously black and superhydrophobic. In this work, we demonstrate a variety of colored superhydrophobic metals. By raster scanning the surface of copper and overlapping a portion of the irradiated area, we create two distinct and geometrically separated nanostructured regions, one forming color, the other inducing superhydrophobicity. Colors forming along the trough of the raster-scanned lines are formed by nanoparticle-induced plasmonic absorption and result in a range of colors from purple to red, depending on the raster scanning speed of the laser. The edges of the raster-scanned area, having been doubly irradiated, form large hierarchical micro/nanostructures which induce superhydrophobicity. Contact angle measurements, spectral examination, and nanoparticle analysis enable us to fully characterize and understand these structures and how they result in dual functionality colored superhydrophobic surfaces.

1. Introduction

One of the most prolific uses of nanotechnology in history is the use of plasmonic nanoparticles in stained glass. Through alchemic experimentation, medieval artisans discovered that adding gold to molten glass resulted in a red tint and adding silver resulted in a yellow tint. These nanoparticles, suspended in glass, absorb light as it passes through the glass and cause color. This earliest and most basic nanotechnology is still used and is being explored by both scientists and artists alike.

Using femtosecond lasers, scientists are functionalizing materials. Functionalizing structures are those structures that when applied to the surface of a material give the underlying material new properties. Using femtosecond lasers, numerous functionalization's have been demonstrated, such as the formation of superhydrophobic surfaces [1–3], superhydrophilic surfaces [4, 5], and plasmonicly colored surfaces [6, 7]. Not only can laser-induced structures impart singular functionalization, but they have also been demonstrated to impart multiple functionalizations simultaneously. Previously it has been demonstrated that laser-ablated metals can be simultaneously colorized black and be made superhydrophobic [8]. We expand on this work and demonstrate the formation of a range of differently colored superhydrophobic metals. While black superhydrophobic metals can see many applications, colorful superhydrophobic metals will be more commercially appealing. Enabling a variety of colors while maintaining superhydrophobicity, without the need for coatings or paints, enables a far greater range of commercial applications than their black superhydrophobic counterpart.

In this paper, we demonstrate and explain the formation of colorful superhydrophobic Cu. By varying the average incident pulse number per unit area on the Cu surface, we can create a range of colors from purple to red. Through contact angle measurements, spectral examination, and nanoparticle analyses, we reveal that these structures contain two distinct geometrically separated regimes, one enabling superhydrophobicity, and one enabling colorization.

#350002 https://doi.org/10.1364/OME.9.001033
Journal © 2019 Received 2 Nov 2018; revised 23 Dec 2018; accepted 23 Dec 2018; published 7 Feb 2019

Optical Materials EXPRESS

2. Methods

All samples were irradiated using a pulsed Ti-sapphire laser system generating 53fs linearly polarized pulses, at a rate of 1kHz, and at a central wavelength of 800nm. Microstructures were formed on 1mm polished Cu foil samples using single direction raster scanning. Cu samples were mounted vertically on a computer controlled dual axis translation stage. The surface structure of the irradiated samples was studied using a scanning electron microscope (SEM) and a UV laser-scanning confocal microscope (UV-LSCM). Contact angle measurements were conducted using a Kino brand static optical contact angle meter. Spectrophotometer data was collected using a PerkinElmer Lambda 365 system.

Laser parameters were optimized to $5.6 J/cm^2$, with an at focus laser beam width of $120 \mu m$. The laser beam width was calculated as the $1/e^2$ width of the laser beam and is roughly equal the ablation profile left upon the raster scanned surface. Raster scanning was performed with an interline spacing of $100 \mu m$ resulting in an irradiated overlap of $20 \mu m$ between raster scanned lines. During irradiation, the laser beam was p-polarized with respect to the scanning direction. After laser processing, samples were ultrasonically cleaned in distilled water for 30 seconds to remove dust and loosely attached nanoparticles.

3. Results and discussion

3.1. Color and geometry

Figure 1 shows the range of superhydrophobic colors able to be formed on Cu following femtosecond laser processing. This range of colors was achieved by optimizing the laser beam fluence to $5.6 J/cm^2$. After optimization of laser parameters, the surface colors are varied only by changing the scanning speed of the translation stage during femtosecond laser irradiation. Colors formed, and their associated scanning speeds are: orange - 3mm/s, red - 2.5mm/s, pink - 2mm/s, purple - 1.5mm/s, blue - 1mm/s, teal - 0.75mm/s, green - 0.5mm/s, dark green - 0.25mm/s, and black - 0.1mm/s. Figure 1(b) shows the $100 \mu m$ spaced raster scanned lines carved out during laser irradiation for the 3mm/s raster scanned sample. The focused laser beam, being $120 \mu m$ wide at the surface results in a $20 \mu m$ of overlap between raster scanned lines. This overlap forms structures distinct from those of the non-overlapped areas, resulting in two distinct geometrically separated regimes, one forming colors and one forming only black. Figure 1(c) is the height profile for a slice of the surface shown in Fig. 1(b) and shows peaks and troughs that correspond to the edges and center of the raster scanned lines, respectively. Comparing the two images, the black portions of the raster scanned Cu sample correspond to the peaks of the height profile, while the colored portion corresponds to the troughs of the height profile. Thus, the center of the raster scanned lines form various colors based on the scanning speed, while the edges of the raster scanned lines, with their $20 \mu m$ overlap, results in black coloration.

Energy-dispersive X-ray spectroscopy (EDX) was performed to identify if oxidation was the cause of the observed colorations formed on the processed Cu samples. Analysis revealed that within a penetration depth of 300nm, the approximate thickness required for an oxide layer to induce colorization on metals [9–11], there was less than 9% oxygen observed. Therefore, the colorizations observed on the laser irradiated Cu samples within this study are induced by structural formations rather than chemical modification.

3.2. Hydrophobic response

Upon placing a water droplet atop the surface of any of the processed colored samples, it is clear that these femtosecond laser irradiated surfaces are superhydrophobic. Figure 2 shows the hydrophobic response of the laser irradiated samples. As the scanning speed of the laser is increased, the hydrophobic response decreases slightly from a contact angle of 160 degrees to a contact angle of 150 degrees, see Fig. 2(a). Having a contact angle greater than 150 degrees

Optical Materials EXPRESS

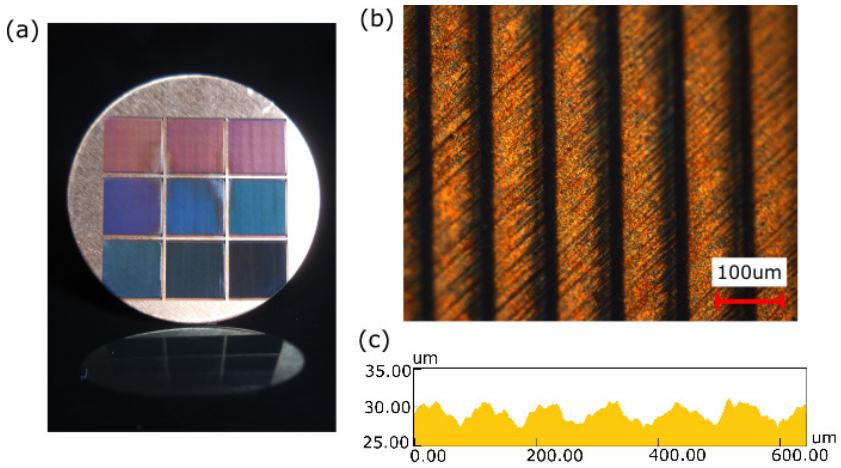

Fig. 1. (a) Photograph of femtosecond laser processed Cu, demonstrating the range of colors able to be formed. (b) Microscope image of the 3mm/s raster scanned Cu surface showing both dark and colored bands. (c) Height profile for a line of image b, illustrating that colored bands of the sample correspond to the troughs of the profile, while dark bands correspond to the peaks of the profile. Angled polishing marks are visible upon the colored bands.

means all samples in our study are superhydrophobic [12]. The observed decrease in hydrophobic response corresponds to a decrease in the depth of the raster scanned lines, see Figs. 2(b) and 2(c). The faster scanning of the laser allows fewer pulses to irradiate the surface of the Cu sample, limiting ablation, which decreases the depth of the raster scanned lines.

It is well known that high surface roughness and high aspect ratio features induce greater hydrophobic responses [8, 13]. Therefore, it is interesting that while hydrophobicity has a linear response to scanning speed, hydrophobicity seems to instead have a logarithmic association to depth. Increasing the ablation depth has diminished returns on the hydrophobic response of the material past a depth of only $10\mu m$.

Figure 2(d) shows a water droplet sitting above a 1mm/s raster scanned sample. The scanned surface strictures can be seen in this image as a saw-toothed periodic dark outline. This image illustrates that the water droplet is sitting solely on the tips of the raster scanned profile. These black irradiated tips are therefore solely responsible for the hydrophobic response of the surface, as the water droplet does not interact with the colorized trough region.

3.3. Spectral response

When viewed under a microscope, both the black and colored stripes of the raster scanned laser irradiated Cu surface are visible. Comprising only 20% of the total surface of the sample, the black lines that form at the peaks of the raster scanned lines are macroscopically unnoticeable at a distance. What is viewed is only the color created in the wide area troughs of the laser irradiated raster scanned lines. Figure 3 shows the spectral response of the laser irradiated samples. Figure 3(a) shows this response in the wavelength range from 200nm to 1,200nm and compares it to an unprocessed control sample. Overall, the total reflectance is much reduced compared to the unprocessed sample. This is most likely due to a combination of internal reflections, Fresnel absorption, and plasmonics resulting from nanoparticle surface features caused by ablation processes following laser irradiation.

Figure 3(b) shows the change in reflectance between the spectral response of the unprocessed sample and that of the various laser irradiated samples. This figure illustrates that electromagnetic absorption by structures formed on the surface of the various Cu samples increases sharply at

Optical Materials EXPRESS

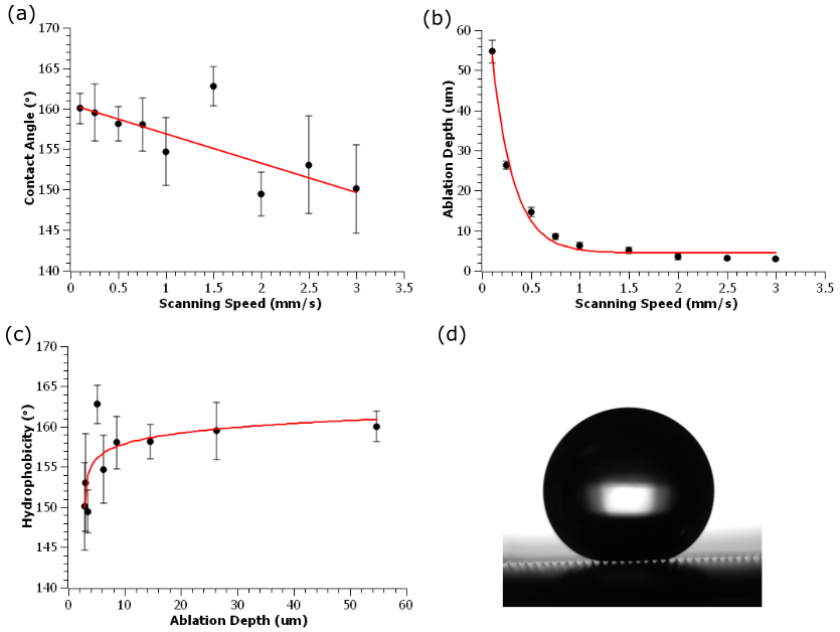

Fig. 2. Hydrophobic response of the laser processed Cu samples. (a) Linear response of scanning speed to contact angle for the irradiated samples. (b) Inverse exponential response of scanning speed to ablation depth for the samples. (c) Logarithmic response of ablation depth to hydrophobicity. (d) Image of a water droplet placed above a 1mm/s raster scanned sample, illustrating that water droplets only contact the tips of the raster scanned structures.

roughly 600nm and broadens as well as redshifts with slower scanning speeds. The broadband absorption observed appears to be bimodal, with peaks at roughly 700nm and 900nm that also redshift with slower scanning speeds. Figure 3(c) is a zoomed in view of Fig. 3(a), highlighting the colored Cu samples' response in the visible spectrum. Figure 3(d) is the same information portrayed in Fig. 3(c) but weighted according to the human eyes luminous response to these frequencies. This weighing of the spectrophotometer data was done by multiplying the spectral response of the Cu sample surface to the CIE 1988 Spectral Luminous Efficiency Function for photopic vision. This shows that even though absorption in the 600nm-720nm range appears to increase linearly with slower scanning speeds, the human eye being incredibly sensitive to frequencies most near the 555nm area sees small fluctuations in this area as much more pronounced and so the colors observed do not simply trend linearly from red to purple. For this reason, 0.25mm/s raster scanned Cu which has the highest overall spectral absorption is not the visibly darkest sample because it has a higher reflectance near 555nm than the visibly darker 0.1mm/s raster scanned sample.

3.4. Morphological analysis

SEM images of the surface of the raster scanned Cu surfaces reveal two distinct regions of particle formation, see Fig. 4(a). The tops of the raster scanned lines are covered in large bulbous nano-covered microstructures, Fig. 4(b), while the troughs are filled with a dense bed of nanostructures, Fig. 4(c). Large and hierarchical micro/nanostructures as formed here have previously been found to cause blackening due to antireflection effects caused by randomly positioned subwavelength particles and surface textures formed after laser irradiation. Additionally, the hierarchical nature of these peak structures has also been found to be ideal for inducing hydrophobicity [8, 14, 15].

Optical Materials EXPRESS

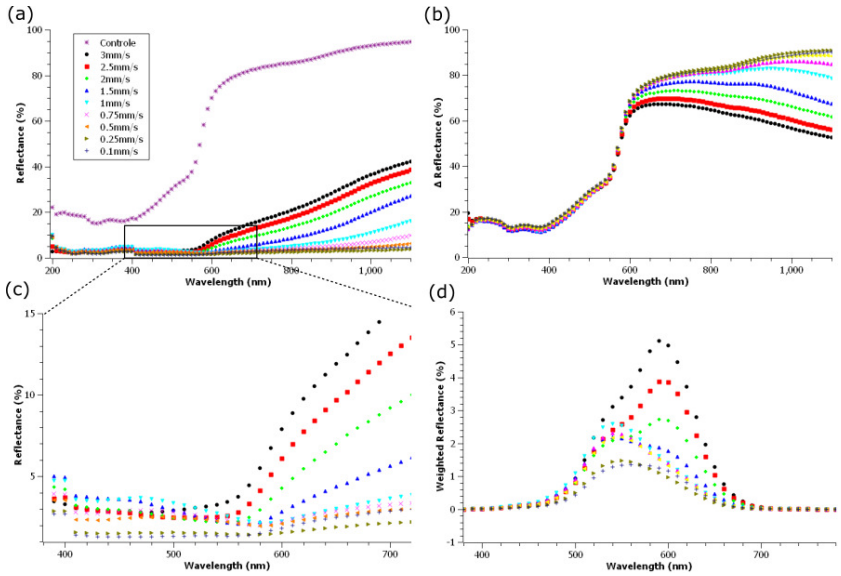

Fig. 3. Spectral responses for pulsed femtosecond laser irradiated Cu surfaces for various raster scanning speeds. (a) Spectral reflectance in the wavelength range from 200nm to 1,200nm. (b) The change in reflectance between an unprocessed sample and that of the various laser irradiated samples. (c) A magnified view of Fig. 4(a), highlighting the visible spectrum. (d) The same information portrayed in figure c but weighted according to the CIE 1988 Spectral Luminous Efficiency Function for photopic vision.

Hierarchical micro/nanostructures increase surface roughness, lowering the overall surface energy. When a material has a very low surface energy, the surface tension of a water droplet will be greater than the adhesion force to the source causing the water droplet to bead up and roll off easily. Due to the Gaussian profile of the laser beam, the local fluence at the edges of the raster scanned lines have a much reduced local fluence when compared to the center of the raster scanned line. This low fluence, along with the double irradiation of laser pulses induced from the overlapped raster scanning method employed results in these large and bulbous nano-covered microparticles. As has been observed previously, large numbers of pulses at relatively low fluences can give rise to these types of structures [8, 16]. Continuous low fluence pulses will induce melting dynamics that can grow or amalgamate nanoparticles, forming larger structures. Ablation processes also present will cause nanoparticle redisposition atop these amalgamated melted nanoparticles, ultimately forming hierarchical nano-covered microstructures. The slight asymmetry of nanoparticles forming along the raster scanned lines is most likely due to a slight asymmetry in the beam profile of the femtosecond laser system employed.

Located in both geometric regimes (e.g. the peak and trough), are parallel periodic lines known as laser induced periodic surface structures (LIPSS). These structures are thought to be formed from the interference between incident laser light and excited surface plasmon polaritons [17]. The LIPSS here formed have a period of 780nm, and become more pronounced with slower scanning speed. Though these LIPSS certainly have a plasmonic response, i.e., they can excite propagating surface plasmon polaritons (SPPs), they are not considered to greatly affect the overall colorization of the surface. If the observed color were due to SPPs excited by these ripples, then one would expect to see an angle dependent iridescence.

Figure 5 shows analyses, as well as more detailed views of the nanostructures formed in the trough region of the raster scanned lines. As scanning speed decreases, nanoparticles appear more frequently and grow from nearly 19nm to 25nm in radius, see Fig. 5(g). As previously discussed,

Optical Materials EXPRESS

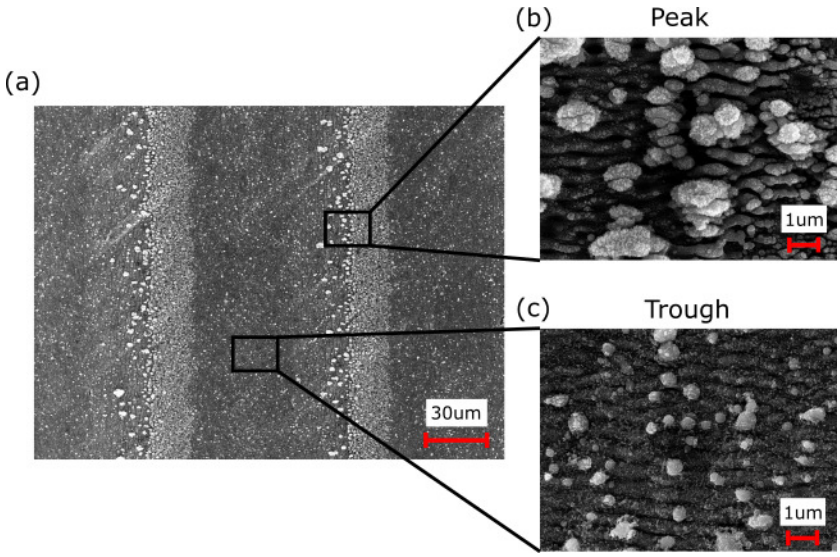

Fig. 4. SEM images of a 1.5mm/s raster scanned Cu surface. (a) SEM image of the large scale raster scanned lines formed on the surface of Cu after laser irradiation. (b) Magnified SEM image showing the bulbous and hierarchical microstructures formed at the peaks of the raster scanned lines. (c) Magnified SEM image showing the finer nanostructures formed within the troughs of the raster scanned lines.

larger nanoparticles have been found to induce darkening of metal surfaces [18, 19]. The increase in large nanoparticle size observed clearly correlates to the overall reduced reflectance observed for slower scanning speeds. Along with average radius, the overall density of particles simultaneously increases as scanning speeds decrease, see Fig. 5(h). The end result is an overall decrease in interparticle spacing as scanning speeds decrease, see Fig. 5(i).

The correlation between scanning speed and broadness of the absorption band can be understood using the plasmon hybridization model. For slower scanning speeds, larger nanoparticles are created and the inter-particle distance decreases. Consequently, the near-field coupling between the nanoparticles hybridize the plasmonic modes which generates resonance at longer wavelengths. Since the nanoparticles are randomly distributed, the convolution of red-shifted hybridized modes creates a broadband mode. In addition, the increase in the nanoparticle size results in an increase in the near-field strength and spatial extension which leads to even stronger hybridization [20].

4. Conclusions

In this paper, we have demonstrated and explained the formation of colorful superhydrophobic copper. By varying the average incident pulse number per unit area on the copper surface, we created a range of colors from purple to orange. Through contact angle measurements, spectral examination, and nanoparticle analyses, we reveal that these structures contain two distinct geometrically separated regimes, one enabling superhydrophobicity, and one enabling colorization. Large and hierarchical structures at the peaks of the raster scanned lines instill superhydrophobicity, while large area, densely packed, nanoparticles located within the trough of the raster scanned lines excite plasmonic colorization. Due to the geometric separation in functionalizing regimes, the hydrophobicity induced at the peaks of the processed sample can protect the color inducing nanoparticles' integrity located in the lower portions of the sample, increasing the colorization effects longevity.

Optical Materials EXPRESS

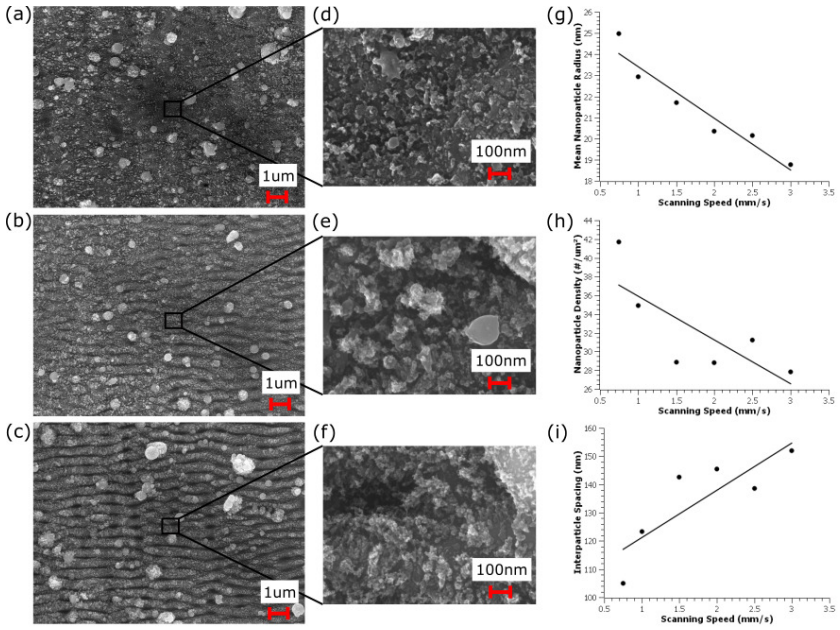

Fig. 5. SEM photos and analysis of nanoparticles formed within the troughs of laser irradiated raster scanned lines on Cu. Figures 6(a), 6(b), and 6(c) show SEM photos of 3mm/s, 2mm/s, and 1mm/s laser irradiated samples, respectively. Figures 6(d), 6(e), and 6(f) show magnified views of SEM photos in Figs. 6(a), 6(b), and 6(c), respectively. Figures 6(g), 6(h), and 6(i) show the relation between scanning speed and nanoparticle radius, nanoparticle density, and interparticle spacing, respectively.

Funding

Bill and Melinda Gates Foundation (OPP1157723); US Army Research Office (ARO) (W911NF-15-1- 0319).

References

1. A. Vorobyev and C. Guo, "Multifunctional surfaces produced by femtosecond laser pulses," J. Appl. Phys. **117**, 033103 (2015).
2. T. Baldacchini, J. E. Carey, M. Zhou, and E. Mazur, "Superhydrophobic surfaces prepared by microstructuring of silicon using a femtosecond laser," Langmuir **22**, 4917–4919 (2006).
3. B. Wu, M. Zhou, J. Li, X. Ye, G. Li, and L. Cai, "Superhydrophobic surfaces fabricated by microstructuring of stainless steel using a femtosecond laser," Appl. Surf. Sci. **256**, 61–66 (2009).
4. A. Vorobyev and C. Guo, "Water sprints uphill on glass," J. Appl. Phys. **108**, 123512 (2010).
5. A. Vorobyev and C. Guo, "Femtosecond laser modification of material wetting properties: a brief review," Sci. Adv. Mater. **4**, 432–438 (2012).
6. M. S. Ahsan, F. Ahmed, Y. G. Kim, M. S. Lee, and M. B. Jun, "Colorizing stainless steel surface by femtosecond laser induced micro/nano-structures," Appl. Surf. Sci. **257**, 7771–7777 (2011).
7. A. Y. Vorobyev and C. Guo, "Colorizing metals with femtosecond laser pulses," Appl. Phys. Lett. **92**, 041914 (2008).
8. A. Y. Vorobyev and C. Guo, "Direct femtosecond laser surface nano/microstructuring and its applications," Laser & Photonics Rev. **7**, 385–407 (2013).
9. Z. Li, H. Zheng, K. Teh, Y. Liu, G. Lim, H. Seng, and N. Yakovlev, "Analysis of oxide formation induced by uv laser coloration of stainless steel," Appl. Surf. Sci. **256**, 1582–1588 (2009).
10. S. O'Hana, A. J. Pinkerton, K. Shoba, A. Gale, and L. Li, "Laser surface colouring of titanium for contemporary jewellery," Surf. Eng. **24**, 147–153 (2008).
11. A. P. Del Pino, J. Fernández-Pradas, P. Serra, and J. Morenza, "Coloring of titanium through laser oxidation: comparative study with anodizing," Surf. Coat. Technol. **187**, 106–112 (2004).
12. S. Wang and L. Jiang, "Definition of superhydrophobic states," Adv. Mater. **19**, 3423–3424 (2007).

Optical Materials EXPRESS

13. A.-M. Kietzig, S. G. Hatzikiriakos, and P. Englezos, "Patterned superhydrophobic metallic surfaces," Langmuir **25**, 4821–4827 (2009).
14. M. V. Rukosuyev, J. Lee, S. J. Cho, G. Lim, and M. B. Jun, "One-step fabrication of superhydrophobic hierarchical structures by femtosecond laser ablation," Appl. Surf. Sci. **313**, 411–417 (2014).
15. Y. Su, B. Ji, Y. Huang, and K.-c. Hwang, "Nature's design of hierarchical superhydrophobic surfaces of a water strider for low adhesion and low-energy dissipation," Langmuir **26**, 18926–18937 (2010).
16. A. Vorobyev and C. Guo, "Femtosecond laser structuring of titanium implants," Appl. Surf. Sci. **253**, 7272–7280 (2007).
17. J. Bonse, S. Hohm, S. V. Kirner, A. Rosenfeld, and J. Kraijger, "Laser-induced periodic surface structures: a scientific evergreen," IEEE J. Sel. Top. Quantum Electron. **23** (2017).
18. A. Vorobyev and C. Guo, "Femtosecond laser blackening of platinum," J. Appl. Phys. **104**, 053516 (2008).
19. A. Y. Vorobyev, V. Makin, and C. Guo, "Brighter light sources from black metal: significant increase in emission efficiency of incandescent light sources," Phys. Rev. Lett. **102**, 234301 (2009).